Breakdown and Self-healing in Tantalum Capacitors

Alexander Teverovsky

Jacobs Technology Inc.
NASA/GSFC, code 562, b.22, rm. C163
Greenbelt, MD 20771, USA

Abstract

Reliability of tantalum capacitors depends on the efficiency of self-healing that restores parts after breakdown. In this work, different types of polymer and MnO_2 cathode capacitors have been tested for scintillation breakdown using a constant current stress (CCS) technique modified to allow detection of amplitudes and duration of current spikes. Monitoring of leakage currents with time under bias is used to assess the effect of scintillations. The appearance and composition of damaged sites have been examined after deprocessing and cross-sectioning. Thermal processes during scintillations have been analyzed, a mechanism of breakdown based on growth of conductive filaments in the dielectric suggested, and self-healing processes in polymer and MnO_2 cathode capacitors discussed.

Index Terms – **tantalum capacitor, electric breakdown, self-healing, damage**

1 INTRODUCTION

Dielectric layers in tantalum capacitors are formed by anodic electrolytic oxidation of porous tantalum pellets. For capacitors rated from 6 to 50 V the thickness of the dielectric is from 30 to 450 nm therefore at rated voltages tantalum capacitors are operating at high electric fields, in the range from 100 to 200 V/μm. These fields are only 2-3 times below the breakdown fields in Ta2O5 dielectrics that are in the range from 320 to 420 V/μm [1]. Thermochemical processes in the dielectric can cause failures at voltages substantially lower than the breakdown voltage (VBR) and the time to failure in tantalum capacitors can be simulated using a time-dependent dielectric breakdown (TDDB) model [2]. However, due to the self-healing that allows for a fast termination of breakdown and prevention of significant damage to the dielectric, tantalum capacitors can assure long-term operation in variety of reliability demanding applications.

A mechanism of self-healing in MnO_2 capacitors is associated with oxygen reduction in the cathode layer caused by a local overheating and isolation of the breakdown site with high-resistive Mn_2O_3/Mn_3O_4 compositions [3]. Although the mechanism of self-healing in MnO_2 capacitors is commonly accepted, the effect of scintillations on characteristics of tantalum capacitors has not been sufficiently analyzed yet. There is lack of data related to the duration and amplitude of scintillation spikes and information regarding location, appearance and composition of the damaged sites.

Even less is known about self-healing in chip polymer tantalum capacitors (CPTCs) where MnO_2 cathode is replaced with a layer of a conductive polymer, typically poly(3,4-ethylenedioxythiophene) polystyrene sulfonate (PEDOT:PSS) compositions. J.Prymak and co-workers assumed that the self-healing activity in CPTCs involves changes in the conductivity of the fault site, or a break in the contact by evaporating the polymer. It was suggested that this activity requires much less energy than for MnO_2 capacitors [4]. T.Zednicek also explained self-healing in CPTCs by formation of voids caused by evaporation or peeling-off the conductive polymer at the breakdown site [5]. Y.Freeman attributed self-healing to the separation between PEDOT and PSS molecules in the vicinity of defect sites in the dielectric. It was assumed that the separation was caused by high current density and rising temperature that increases resistance of the polymer and decreases leakage currents in the parts [3].

In spite of the importance of self-healing for assuring reliable operation of tantalum capacitors, the associated processes and mechanisms have not been studied sufficiently and need more analysis. In this work, different types of polymer and MnO_2 capacitors have been tested for scintillation breakdown using a constant current stress (CCS) technique modified to allow detection of current spikes during breakdown. Leakage currents were monitored with time at rated voltages to assess the efficiency of self-healing. Damaged sites were localized using infrared camera and their appearance analyzed after deprocessing and cross-sectioning. Thermal processes during scintillations have been modeled to better understand mechanisms of damaging, self-healing and post-scintillation behavior of the parts. Mechanism of breakdown in MnO_2 and polymer tantalum capacitors have been suggested and self-healing processes discussed.

2 EXPERIMENT

Measurements of breakdown voltages in capacitors were carried out using a CCS technique [2] that has been modified to detect voltage variations during scintillation events and the shape of the power supply (PS) current spikes. Figure 1a shows a schematic of the test set-up. A source measurement unit (SMU), typically Keithley 2400, in a constant current mode was used to charge a capacitor under test that had a 10 ohm current sense resistor connected in series. An oscilloscope that was trigged by the breakdown event was used to monitor voltage variations across the capacitor and PS currents by voltage measurements across the sense resistor. Test parameters, including the level of charging current and duration of the test were controlled by a PC that was also used to record variations of voltage with time of charging and oscilloscope data. The level of charging currents was selected to charge capacitors to the rated voltage within a few seconds. The breakdown voltage was determined as maximum on the *V-t* curves.

Due to self-healing, the voltage across the part that drops during the scintillation event starts increasing again and the process can be repeated (Figure 1b). If the part remains shorted or voltage does not increase at the same rate as initially, the part does not self-heal and such scintillations are considered damaging.

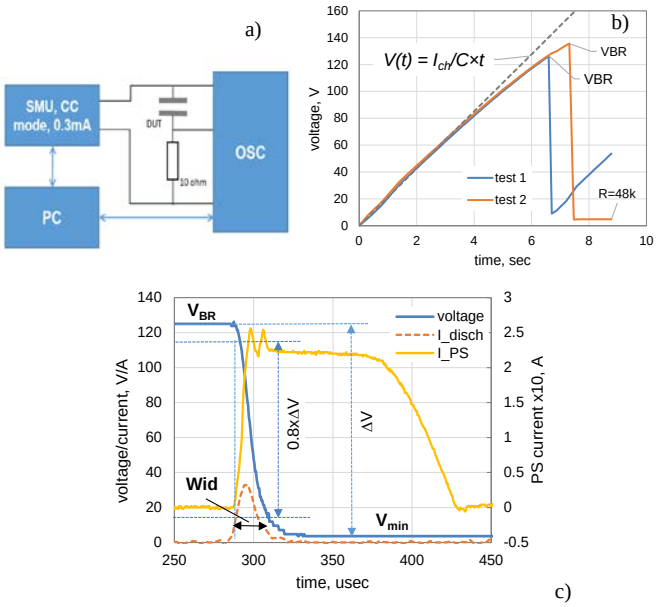

Figure 1. Schematic of the test set-up (a) and typical results of CCS testing at 100 μA (b, c) for a self-healing (test 1) and damaging (test 2) scintillation events in a 4.7 μF 50 V MnO_2 capacitor that resulted in a short circuit failure at 48k. Figure (c) is an example of oscilloscope data showing *V-t* and I_{PS}-*t* curves and discharge currents calculated per Equation (1). The width of the spike, *Wid*, is determined as a time for voltage to decrease from V_{BR} - 0.1×ΔV to V_{min}+0.1×ΔV, where ΔV=V_{BR}-V_{min}.

A current flowing through a capacitor during breakdown is a sum of the PS current, I_{PS}, and internal current caused by discharging of the capacitor, I_{disch}. The discharge current calculated as a derivative of the voltage variations during breakdown:

$$I_{disch}(t) = C \times {}^{dV(t)}/_{dt}. \quad (1)$$

An example of voltage and PS current variations detected by an oscilloscope during a scintillation breakdown is shown in Figure 1c. Scintillation events were characterized by the breakdown voltage, minimal voltage before self-healing, V_{min}, and the width of the discharge, *Wid*, determined as shown in Figure 1c.

PS current spikes had typically a trapezoid shape with the amplitude truncated at ~0.22 A and the width in the range from 50 to 300 μsec. Experiments with different power supplies and a simulation of breakdown by external short circuits showed that the shape and amplitude of PS current spikes depend on the dynamic characteristics of the power supply used and do not reflect self-healing processes in the parts. Apparently, the time for self-healing is greater that the duration of PS current spike.

Various groups of MnO_2 and polymer capacitors from 6.8 μF to 470 μF rated at voltages from 6.3 V to 35 V were used to evaluate the effect of the type of cathode materials on scintillation breakdowns and self-healing capability of the parts. The latter was assessed by the proportion of capacitors damaged after the first scintillation test.

Each group had typically from 10 to 20 samples and was characterized by distributions of V_{BR} and V_{min} (Weibull distributions), durations of scintillation events, *Wid*, (log-normal distributions) and proportion of damaged capacitors, *d*.

Characteristics of capacitors were measured before and after CCS testing. Results showed that for all parts, the least sensitive to scintillations characteristics are capacitance and equivalent series resistance (ESR), and the most sensitive is leakage current.

3 TEST RESULTS

3.1 BREAKDOWN VOLTAGES AND SCINTILLATION TIMES

Figure 2a shows variations of average values of characteristic breakdown voltages calculated for several lots of MnO_2 and polymer capacitors with the voltage rating (VR). Considering the spread of the data, there is no significant difference in VBR between CPTC and MnO_2 capacitors with similar ratings. On average, V_{BR} is 2.7 times greater than VR for both type of capacitors. However, the ratio V_{BR}/VR is greater than the average (~3.5) for 6.3 V capacitors and lower (~2.5) for 35 V capacitors. This is consistent with our previous results for MnO_2 capacitors [6] and is likely related to a greater concentration of defects in thicker Ta_2O_5 dielectric layers [3].

The slopes of Weibull distributions of breakdown voltages, β, on average are substantially larger for polymer than for MnO2 capacitors (see Figure 2b). Tighter distributions for polymer capacitors indicate smaller low-voltage tails, therefore a lesser probability of having defects in the dielectric. This is likely due to lower process temperatures for polymer technology (≤ 180 ºC) that creates less stressful conditions in the process of cathode formation compared to MnO_2 technology that requires from 250 to 350 ºC.

Average scintillation times, are varying from ~0.25 ±0.2 msec for 35 V to ~1.25 ±1 msec for 6.3 V MnO_2 capacitors (see Figure 2c). For polymer capacitors rated to 16 V and above, these values are 2 to 7 times greater. Discharge times are similar for both types of capacitors rated to 6.3 and 10 V, but the spread

of *Wid* values is large, ~ 1 msec for 6.3 V to ~ 0.5 msec for 10 V capacitors.

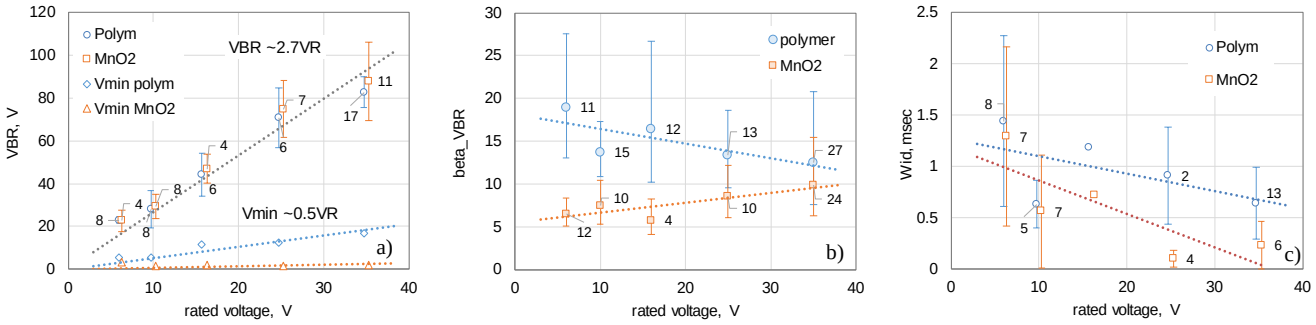

Figure 2. Variations of breakdown and minimal voltages (a), median values of the slopes (β_{VBR}) of Weibull breakdown distributions (b), and scintillation times (c) for MnO_2 and polymer capacitors with the rated voltage. Digits at the marks correspond to the number of tested lots.

3.2 DAMAGING SCINTILLATIONS

A proportion of capacitors damaged during scintillation events, *d*, for 5 lots of MnO_2 and 11 lots of polymer capacitors rated to 35 V is shown in Figure 3a. The value of *d* varies from lot to lot substantially, but on average, it is much less for MnO_2 (d_{avr} = 11.5% at a standard deviation of 14.6%) than for polymer capacitors (d_{avr} = 88.3% at a standard deviation of 14.3%).

Average values of *d* for 41 lots of polymer and 34 lots of MnO_2 capacitors with different VR are plotted in Figure 3b. For capacitors rated to ≥16 V, the average proportion of damaged parts is 2 to 4 times greater for polymer than for MnO_2 capacitors, but for lower voltages, the spread of data increases, so the difference is not significant.

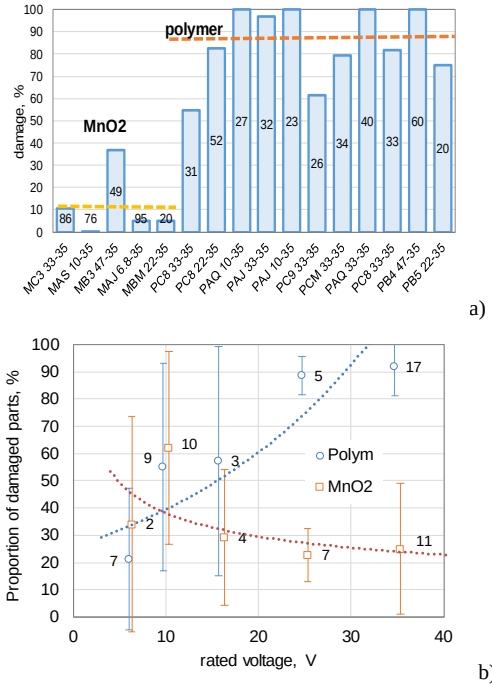

Figure 3. Proportion of damaging scintillations in different lots of MnO_2 and polymer capacitors rated to 35 V (a) and variations of average values of *d* with the rated voltage (b). Digits in (a) indicate the number of tested samples in a lot, and dashed lines correspond to the average values of damaged polymer and MnO_2 capacitors. Digits in (b) indicate the number of tested lots and the error bars standard deviations. Different lots in (a) were marked by three letters indicating type of the cathode material (M for MnO_2 and P for polymer), manufacturer (A, B, or C), and the third letter or number reflects the type of capacitors.

Discharging during scintillation events in polymer capacitors takes more time compared to MnO_2 capacitors. This indicates a lower average power of scintillations in CPTCs, and at similar VR, the probability of damaging should have been less than in MnO2 capacitors. However, majority of polymer capacitors fail the first scintillation test. These failures were due to substantial variations of the discharge power with time during scintillations. Examples of such events for PB4 47 µF 35 V capacitors are shown in Figure 4. Sample SN8 had maximum discharge rate at the beginning of the process that resulted in a 100 µsec, 30 A current spike and a short circuit failure at 4.6k that stabilized after hundreds of milliseconds. For SN13, the discharge lasted ~2 msec, but had two current spikes. One at the beginning that resulted in a relatively small 10 A, 100 µsec spike and another, larger spike of 88 A, 50 µsec at the end of the discharging process. Similar to these results, in general, capacitors exhibiting short, high current spikes have a larger probability of causing damage and the greater the power of the spikes, the more severe damage they cause.

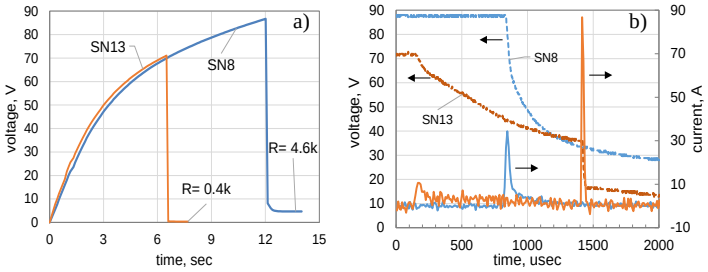

Figure 4. Variations of voltage with time during CCS testing at 1 mA (a) and discharge current spikes (b) for different samples of polymer 47 µF 35 V capacitors.

Examples of power variations during scintillations in MnO_2 and polymer capacitors are shown in Figure 5. The amplitudes of power spikes during scintillations varied from hundreds of watts to dozens of kilowatts, and their duration was in the range from 2 to 5 µsec. The less powerful spikes that did not cause shorting failures had amplitudes below a few hundreds of watts and durations from 10 to 100 µsec.

Some MnO_2 capacitors were functional even after being damaged by a breakdown that resulted in chip-outs in the case revealing destruction of cathode layers and exposing tantalum pellets. These parts did not fail short circuit and were able to

sustain consecutive scintillation tests indicating high self-healing efficiency that can be provided by the MnO_2 technology. On the other hand, several MnO2 330 µF and 470 µF capacitors ignited during CCS testing and their burning lasted for several seconds after the test was terminated. This suggests that energy stored in large value capacitors might be sufficient for triggering exothermic oxidation of tantalum and ignition by a scintillation event even when parts are used in high impedance circuits with a limited current from the power supply. In this regard, large CV value CPTCs are more reliable compared to MnO_2 cathode capacitors. Note that the MnO_2 capacitor passed the first test, but failed the second one (Figure 5a). However, the polymer capacitor failed the first test at 25k at ~ 20 V, but the voltage increased to more than 80 V during the second test (Figure 5b).

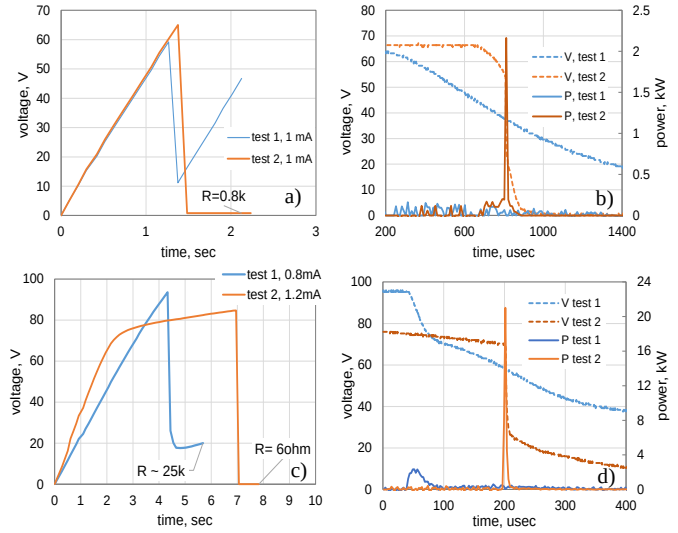

Figure 5. Examples of CCS testing (a, c) and variations of voltage and power during consecutive scintillation tests (b, d) for 22 µF 35 V MnO_2 (a, b) and 33 µF 35 V (c, d) polymer tantalum capacitors.

This indicates that recovery of polymer capacitors damaged by scintillations occurs differently compared to MnO_2 capacitors. Figure 6 shows results of four consecutive CCS tests for a sample of PC8 22 µF 35 V capacitors. This part failed at 54k after the first scintillation with voltage stabilizing at ~ 27 V. However, voltage continued increasing above 30 V during the second and the third tests, although at a lower rate than initially, which is explained by relatively large, but decreasing with consecutive tests leakage currents. During the fourth test, the rate of voltage increase was similar to the initial suggesting that the leakage currents decreased to the microampere range, and the part reached voltages higher than the initial breakdown. After that, the part failed at ~ 6k. The rate of voltage discharge during the fourth test was greater than during the first one resulting in a more powerful breakdown with a spike of 7 kW during 100 µsec compared to 2 kW for 200 µsec initially.

3.2 EFFECT OF SCINTILLATIONS ON LEAKAGE CURRENTS

Variations of leakage currents with time at room temperature for 6.8 µF 35 V MnO_2 capacitors after CCS testing are shown in Figure 7a. Note that currents in virgin capacitors were below 0.1 µA for 100 hours of testing, but scintillations increased currents approximately an order of magnitude and three samples, SN9, 10, 51 and 54 were unstable exhibiting current spikes. These spikes indicating additional scintillations appeared after a few hours of testing and would not be detected by regular screening procedures. Apparently, excessive currents and scintillations might develop in damaged capacitors with time at relatively low voltages, which is in agreement with the TDDB model of failures [2].

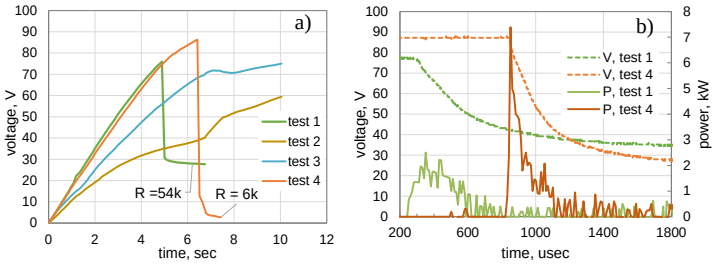

Figure 6. Four consecutive CCS tests at 0.5 mA for a 22 µF 35 V capacitor (a) and voltage discharge and power spikes during the initial and final tests (b).

Figure 7b displays result of 800 hours life testing at 85 ºC 35 V for a group of 15 non-stressed samples and 47 capacitors stressed by three non-damaging scintillation breakdowns. For this test, the parts with anomalies shown in Figure 7a have been removed from the population. All virgin capacitors at 85 ºC had leakage currents well below 1 µA, whereas capacitors that experienced scintillation breakdowns had more than two orders of magnitude greater and increasing with time currents. Approximately 40% of the stressed capacitors increased leakage currents above the specified limit of 24 µA by the end of life testing, whereas leakage currents in the virgin parts remained below 0.5 µA.

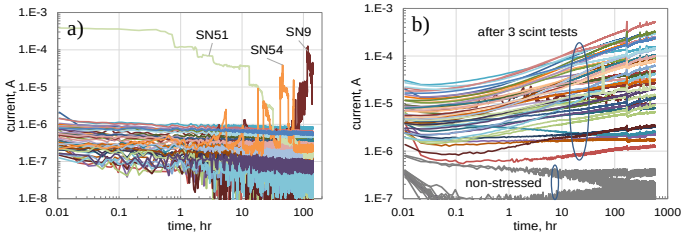

Figure 7. Variations of leakage currents in MnO2 6.8 µF 35 V with time at 35 V and room temperature (a) and at 85 ºC (b). Figure (a) shows results for capacitors stressed by three scintillation tests, and Figure (b) – for the stressed and non-stressed capacitors.

Similar results indicating increased leakage currents and the rate of degradation were obtained for other types of MnO_2 capacitors that were not shorted and appeared self-healed during CCS testing. Apparently, scintillations degrade performance even for self-healed tantalum capacitors.

Leakage currents in CPTCs behaved differently. As an example, Figure 8 shows results of testing of polymer and MnO_2 22 µF 35 V capacitors before and after scintillation testing. Both types of capacitors were produced by the same manufacturer using the same processes and materials except for the formation of cathode layers. Based on CCS results, 15 out of 20 polymer and none out of 20 MnO_2 capacitors were damaged during scintillation testing. Five non-damaged and three damaged polymer capacitors were used for testing shown in Figure 8. A substantial, increase of currents for damaged

polymer capacitors was expected. However, leakage currents in non-damaged polymer capacitors also increased substantially, ~ 100 times, which is greater than the increase for MnO_2 capacitors (~ 10 times). Also, currents in all CPTCs, including damaged parts, decreased gradually with time and reduced after 20 hours of testing to the level close to initial. Contrary to polymer, MnO_2 capacitors had a tendency of increasing currents with time under bias.

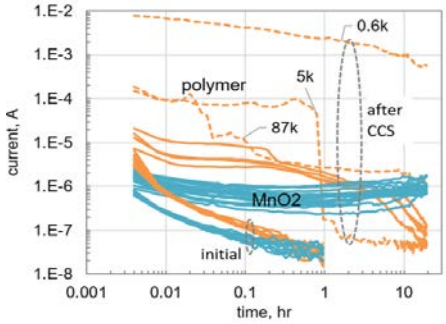

Figure 8. Initial and post-CCS leakage currents in MnO_2 and polymer 22 µF 35 V capacitors from the same manufacturer. Dashed lines correspond to capacitors that failed CCS test at the indicated resistances.

3.3 FAILURE ANALYSIS

Six samples of MnO_2 and 8 samples of polymer capacitors damaged by CCS testing have been deprocessed by removing plastic case and cathode layers or cross-sectioned to reveal location and appearance of the breakdown sites. The structure and compositions of damaged areas were analyzed using scanning electron microscopy (SEM) and energy dispersive spectroscopy analysis (EDS). Before deprocessing or cross-sectioning, position of the damage was detected using an infra-red camera at a dissipating power in the range from 20 to 120 mW. A detailed description of design and material used in tantalum capacitors can be found elsewhere [3, 5].

Figures 9 and 10 show examples of damaged sites for MnO_2 and polymer capacitors. Common features of damages in for both types were location on the surface of pellet, size of the damaged area in the range from 100 to 200 µm, presence of voids in cathode layers, and structural changes in the pellet. The latter appeared as fused tantalum oxide particles and large non-stoichiometric areas of TaO_x, x < 2.5. Multiple adjacent damaged sites with a size of dozens of micrometers were detected in several samples of both types of capacitors (see for example Figure 10a).

Specifics of damage sites was oxygen reduction in the manganese oxide (MnO_x, x<1.5) for MnO_2 capacitors and presence of solidified silver (likely from melting of silver epoxy) in some locations of damages in polymer capacitors. Evidences of solidified tantalum particles indicate that temperature during scintillations can rise up to ~3000 ºC.

4 DISCUSSION

4.1 ENERGY AND POWER OF DISCHARGE

The energy released during a scintillation breakdown originates from the energy stored in the capacitor itself, E_C, and energy provided by the power supply, E_{PS}:

$$E = E_C + E_{PS} \approx 0.5CV_{BR}^2 + I_{PS}V_{BR}W_{PS} \quad (2)$$

where C is the capacitance, I_{PS} = 0.22 A (for SMU K2400) is an average PS current during the spike, and W_{PS} ~ 100 to 200 µsec is the width of PS spike.

Calculations at $V_{BR} = 2.7 \times VR$ for capacitors from 3.3 to 330 µF rated to different voltages show that E varies from 0.2 mJ for 4 V 3.3 µF capacitors to more than 300 mJ for 330 µF 16 V capacitors (see Figure 11a). The energy stored in capacitors is orders of magnitude greater than from the power supply, and even for a relatively low value, 3.3 µF 4 V capacitors it is more than an order of magnitude greater than E_{PS}.

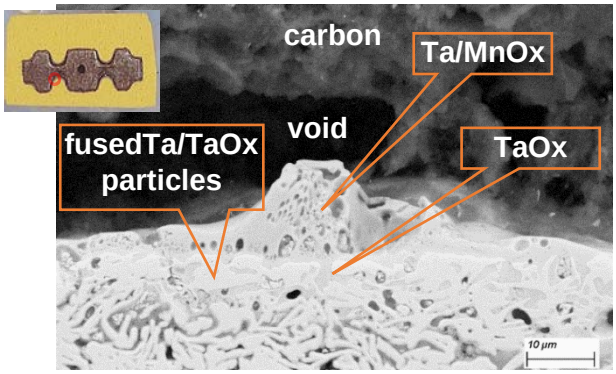

Figure 9. A damaged site in a 6.8 µF 35 V capacitor that failed scintillation testing at 240 ohm. The insert shows an optical image of a cross-section with location of damage on the surface of the flute-like shaped pellet.

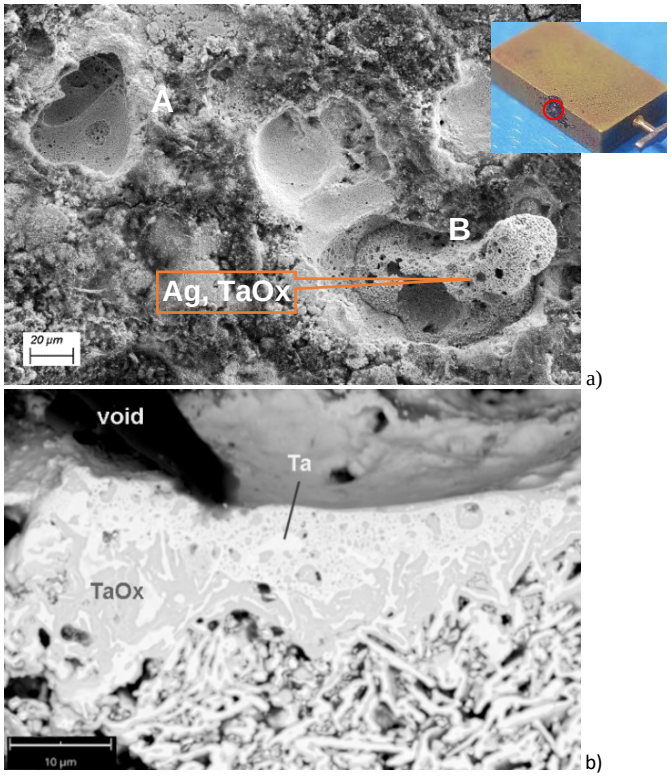

Figure 10. Two damaged sites (A and B) in a polymer 47 µF 35 V capacitor that failed after the first scintillation event at 1ohm (a) and cross-section of a 33 µF 35 V capacitor that failed short circuit at 0.4 ohm (b). Elemental analysis of area B revealed excessive amount of silver. The insert shows location of the damage revealed after deprocessing.

At adiabatic conditions, the whole discharge energy goes for heating up of a certain volume of the pellet. Assuming this

volume is a sphere of radius r, the temperature increase, ΔT, can be calculated from the balance between electrical and heat energy:

$$0.5C(V_{BR}^2 - V_{min}^2) = v\rho\gamma(c\Delta T + C_f) \quad , \qquad (3)$$

where v is the volume of the sphere, ρ is the specific density, c is the specific heat capacity, and C_f is the heat of fusion for tantalum. Characteristics of materials used for calculations per Equation (3) are shown in Table 1.

The table shows also critical temperatures associated with different structural and phase changes in the materials: melting temperature of tantalum, 3017 ºC, melting of Ta2O5, 1870 ºC, oxygen reduction in MnO_2, 535 ºC, and decomposition of conductive polymer, 290 ºC. The latter value was determined in [7] using thermogravimetric analysis (TGA) and differential scanning calorimetry (DSC) for different PEDOT-based compositions used as cathode materials in tantalum capacitors.

Table 1. Characteristics of materials used.

Characteristic	Ta	Ta2O5	MnO2	Polym	Ref
Specific heat capacity, *J/kg_K*	140		630		[8]
Specific density, *g/cm³*	16.7	8.2	5	~1	
Heat of fusion, *J/kg*	176				
Thermal conductivity, *W/m_K*	58		0.2-0.5	~0.2	[9, 10]
Critical temperature, *ºC*	3017	1870	535	290	[3, 7]

Estimations show that the amount of heat that is necessary to increase temperature of the dielectric and cathode layers is negligible compared to the one that is required to heat-up the tantalum pellet. The energy required to melt a sphere of tantalum pellet of radius r, Q_{Ta}, reach the temperature that would cause melting of tantalum oxide, Q_{Ta2O5}, or cause decomposition of manganese oxide, Q_{MnO2}, or polymer, Q_{polym}, is shown in Figure 11b. The energy required to reach melting point of tantalum is substantially greater than the additional energy necessary for melting. For this reason, the values of Q_{Ta2O5}, Q_{MnO2}, and Q_{polym}.are just proportional to the relevant critical temperatures.

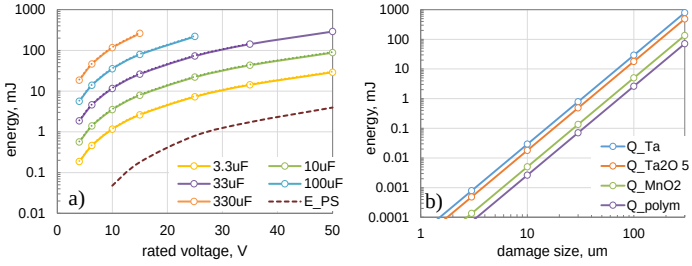

Figure 11. Variations of the energy released during scintillation breakdown for capacitors rated from 3.3 to 330 µF and voltages from 4 to 50 V (a) and relationship between the energy necessary to reach the critical temperature and size of the damage (b). The dashed line in figure (a) indicates the energy provided by the power supply used for CCS testing.

The energy dissipated during scintillation breakdowns is sufficient to damage a relatively large area of the pellet. At breakdown voltages, a 33 µF 35 V capacitor can store ~150 mJ and bring a sphere of tantalum with a size of ~200 µm to the melting temperature. This energy is also sufficient to reach the temperature necessary for oxygen reduction in MnO_2 or to destroy a polymer cathode with a sphere of more than 300 µm. These estimations are in agreement with results of failure analysis showing that damages had a size of ~ 200 µm.

Breakdown during surge current testing (SCT) of tantalum capacitors occurs at the surface of the pellet, and for this reason, manufacturers are using special procedures to increase the thickness of the oxide in the shell areas of the pellet [6]. A fast voltage rise during SCT does not allow increasing voltage across dielectric for the in-bulk areas thus explaining the surface location of breakdown. However, during CCS tests, the voltage rises slowly, which makes possible breakdown in the bulk of the pellet. To understand why surface is still preferable place for breakdown during CCS testing, we need to consider constriction resistances during scintillation breakdown.

Holm's equation [11] for a contact resistance between dissimilar materials can be used to estimate the constriction resistance of a damage of radius r located in the bulk of the pellet:

$$R = \frac{1}{4r}\left[\frac{\rho_{Ta}}{(1-\gamma)} + \frac{\rho_{cat}}{\gamma}\right], \qquad (4)$$

where ρ_{Ta} and ρ_{cat} are specific resistances of the tantalum and cathode materials and $\gamma \approx 0.5$ is the porosity of the pellet. The resistivity of tantalum, ρ_{Ta} = 1.3E-5 ohm_cm, is more than 4 to 5 orders of magnitude below the cathode materials, ρ_{cat} = 1 to 10 ohm_cm for MnO2 capacitors and 0.1 to 1 ohm_cm for polymer capacitors. Note, that considering a very thin, below 0.1 µm thickness of polymer coating inside the pores of the pellet, its effective resistance that should be used for calculations is 10 to 100 times greater than for MnO_2 capacitors. Estimations show that R exceeds hundreds of ohms even for large damage sizes of ~ 100 µm and will limit the power dissipated at the breakdown site substantially. However, breakdown sites located at the surface of the pellet that is covered with a relatively thick (dozens of µm) cathode layers, have substantially lower resistances facilitating development of breakdown.

Obviously, the resistance of a damaged capacitor is a sum of the constriction resistance and the resistance of the damage site itself. Considering that oxygen reduction in MnO_2 that was detected at the periphery of damaged areas. can insulate the damage, this additional resistance might be large enough for MnO_2 capacitors. A substantial increase of the resistance occurs in both, MnO_2 and polymer capacitors when decomposition of the cathode layers results in a large enough void capping the damage.

A simple one-dimensional model allows for assessments of the temperature on the surface of a sample that experienced an instant energy pulse. For a power pulse amplitude P_0 and duration Δt, the peak temperature rise at the surface of the pellet in adiabatic conditions is [12]:

$$\Delta T = \frac{P_0 \Delta t^{0.5}}{\pi r^2 (\gamma \pi k \rho c)^{0.5}}, \qquad (4)$$

For a given size of the damage, same energy pulses ($P \times \Delta t$ = *const*) result in substantially greater temperatures for shorter spikes. For example, 1 kW 3 µsec spike can increase temperature of a 100 µm site up to 4000 ºC, whereas for a spike of 100 W with duration of 30 µsec the temperature rise will be ~ 1000 ºC. Melting of tantalum can be expected in the first case, whereas only reduction of oxygen in MnO_2 or decomposition of polymer can be expected in the second case. This is

consistent with experimental data showing that shorter scintillation spikes are more likely to damage capacitors.

The adiabatic assumption is reasonable for fast enough events when the time for temperature spreading over the region is comparable with the duration of the events. The characteristic time of heat diffusion across a sphere of radius r can be estimated as $\theta = {r^2}/{\alpha}$, where α is the thermal diffusivity, that for a tantalum pellet is ~1.2E-5 m^2/sec. Estimations show that scintillation events in the range from 0.1 to 1 msec might result in adiabatic heating for the damage size in the range from 50 to 100 μm, which is close to the sizes of damages revealed during failure analysis.

4.2 MECHANISMS OF BREAKDOWN AND SELF-HEALING

Processes in the dielectric during scintillation breakdowns in tantalum capacitors can be explained by formation and destruction of conductive filaments similar to operation of ReRAMs [13]. At high electric fields, oxygen ions are dragged from the Ta_2O_5 dielectric to the anode leaving oxygen vacancies in the oxide. As a result, vacancies start accumulating at some locations at the cathode surface forming sites from which conductive filaments are growing. The formation of filaments is a stochastic process and multiple filaments with different diameters are likely formed [14]. A micro-scintillation breakdown occurs similar to the switching or resetting of the elements in ReRAMs when the applied voltage is high enough to generate sufficient amount of joule heating and destruct the filaments thermally [15]. This event has a short, in the range of dozens of nanoseconds, duration and is terminated by a partial thermal destruction of the filament without causing damage to the pellet. Due to a short duration and nanometer size of the filaments, micro-scintillations discharge capacitors only partially, so the process continues until multiple events occur (progressive breakdown) to create a macro-scintillation that is detected experimentally during CCS testing. Schematics in Figure12a, b illustrate the process of the filaments' formation and rupture during micro-scintillations.

The initial micro-scintillation facilitates discharging at the close-by filaments due to an increased temperature in the area that decreases breakdown voltages in tantalum capacitors [6]. As a result, a relatively slow breakdown with duration from 0.1 to 1 msec occurs, but the structure of the pellet might remain intact. After such a breakdown, capacitors have normal characteristics and can be considered self-healed. However, the remnants of filaments increase local electric fields in the dielectric, injection of electrons, and post-CCS leakage currents in the parts. Increased concentration of filaments at the defects in the dielectric and combined effect of multiple micro-scintillations might rise the power density to the level sufficient for a physical damage to the structure of the pellet and cathode layers as illustrated in Figure 12c, d.

The filaments in self-healed capacitors continue growing at rated voltages, although at a much lower rate than at pre-breakdown voltages. This growth increases electric fields and leakage currents with time under bias for MnO_2 capacitors. Another factor increasing the rate of degradation compared to virgin capacitors is generation/activation of oxygen vacancies during scintillation events that enhance redistribution of charged oxygen vacancies and reduce the barrier at the cathode/Ta_2O_5 interface [16].

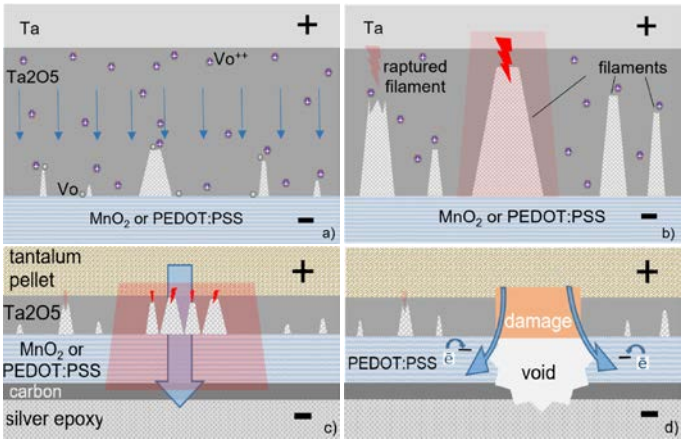

Figure 12. Schematics of breakdown in tantalum capacitors showing formation and growth of conductive filaments (a) and thermal breakdown resulting in rupture of the filaments (b). Figure (c) illustrates a simultaneous breakdown of several filaments resulting in damage to the pellet and heating of a relatively large area at the periphery. Figure (d) shows formation of a void in the cathode layers, and electron trapping in polymer capacitors.

Contrary to MnO_2, leakage currents in polymer capacitors decrease with time under bias after scintillations. Also, some CPTCs can recover after repeat breakdowns. This behavior can be explained assuming that overheating during breakdown dries-out polymer cathode at the periphery of the damage and results in formation of a relatively large area with substantially increased conductivity of the dielectric. This effect is responsible for the anomalous transients phenomena and is specific for CPTCs [17]. Leakage currents in discharged dry polymer capacitors might be comparable or even greater than the charging currents resulting in failures during CCS testing. With time under bias, these currents decrease gradually (seconds to hours) and the parts can recover/self-heal due to electron trapping at the states in the PEDOT:PSS polymers that increases the work function and reduces currents in the dielectric.

Thermal destruction of the filaments results in termination of breakdown, or self-healing in both types, polymer and MnO_2 capacitors. However, the capability of MnO_2 to provide oxygen either by thermal generation or by solid state anodic oxidation [18], results in a compensation of vacancies in the filaments and better self-healing efficiency.

Self-healing in MnO_2 and polymer capacitors is due to a combination of different mechanisms. These mechanisms involve (i) thermo-oxidative destruction of the conductive filaments, (ii) conversion of MnO_2 areas at the damaged site into high-resistive oxides, and (iii) formation of voids in the cathode layers for MnO_2 capacitors. Self-healing in polymer capacitors is due to (i) thermal destruction of the filaments, (ii) formation of voids in the cathode layers, and (iii) trapping of electrons into states in conductive polymers.

Different processes can self-heal capacitors to a different degree and require different times. Destruction of the filaments occurs fast, within dozens of nanoseconds. Oxygen reduction of MnO_2 that forms high-resistive oxides and isolates the damage requires from 0.1 to 1 msec. The time necessary for

formation of the voids is difficult to assess, but based on results of monitoring of PS current spikes, it is likely more than a few milliseconds. Reduction of the anomalous conduction of the Ta_2O_5 dielectric requires much longer time, and depending on the voltage and temperature, the process might take from seconds to hours.

5 SUMMARY

Testing of 34 lots of MnO_2 and 45 lots of polymer tantalum capacitors rated to voltages from 6.3 to 35 V showed that on average, breakdown voltages in polymer and MnO_2 capacitors with the same ratings are close. However, polymer capacitors have tighter distributions of VBR indicating a lesser concentration of defects in the dielectric.

On average, scintillation times are smaller for MnO_2 (*Wid* ≈ 0.4 msec) than for polymer (*Wid* ≈ 1 msec) capacitors. Several short, microsecond range high-power spikes with amplitudes up to dozens of kilowatts might happen during a single scintillation event. Similar spikes create multiple sites with structural damage on the surface of the pellet.

The proportion of capacitors damaged by scintillations varied from lot to lot, but on average was greater for polymer than for MnO_2 capacitors.

Both type capacitors that appeared self-healed during CCS testing have significantly increased leakage currents. Overall, the increase was greater for polymer than for MnO_2 capacitors. However, contrary to MnO_2 capacitors, where leakage currents increased with time under bias, polymer capacitors have a tendency of decreasing currents and recovery even after a significant degradation initially.

Energy stored in capacitors is sufficient to create damaged areas in the range from 100 to 200 μm. The surface location of damaged sites is due to much lower constriction resistances for discharge currents at the surface than in the bulk of the pellet. SEM and EDS analysis of the damaged sites revealed fusing of oxidized Ta particles, formation of large areas of non-stoichiometric TaOx oxide for polymer capacitors or mixture of TaO_x/MnO_x oxides for MnO_2 capacitors.

Breakdown in tantalum capacitors is due to progressive micro-scintillation events caused by the growth of conductive filaments composed of oxygen vacancies. A combined effect of multiple micro-scintillations at a defect site in the dielectric results in structural changes in the pellet and damage to cathode layers.

Several mechanisms with different efficiency and duration occur during self-healing process. For MnO_2 capacitors, these mechanisms include (i) thermo-oxidative destruction of the conductive filaments, (ii) conversion of MnO_2 into high-resistive oxides, and (iii) formation of voids in the cathode layers. Self-healing in polymer capacitors involves (i) thermal rupture of the filaments, (ii) formation of voids in the cathode layers, and (iii) charge trapping in the polymer cathode that decreases anomalous currents caused by drying and discharging during breakdown.

ACKNOWLEDGMENT

This work was sponsored by the NASA Electronic Parts and Packaging (NEPP) program. The author is thankful to Peter Majewicz, NEPP Program manager and Jonathan Pellish, NEPP program deputy manager for support of this task, and Bruce Meinhold, SSAI, chief staff engineer, for a review and discussions. My sincere appreciation to manufacturers of tantalum capacitors for providing samples for this study.

REFERENCES

[1] L. W. McPherson, J. Kim, A. Shanware, H. Mogul, and J. Rodriguez, "Proposed universal relationship between dielectric breakdown and dielectric constant," in *Digest. International Electron Devices Meeting, IEDM '02*, 2002, 8-11 Dec., pp. 633 - 636.

[2] A. Teverovsky, "Scintillation Breakdowns and Reliability of Solid Tantalum Capacitors," *IEEE Transactions on device and materials reliability*, vol. 9, pp. 318-324, 2009

[3] Y. Freeman, *Tantalum and Niobium-Based Capacitors: Science, Technology, and Applications*: Springer, 2017.

[4] J. D. Prymak and M. Prevallet, "Scintillation Testing of Solid Electrolytic Capacitors," in *The 26th symposium for passive components, CARTS'06*, Orlando, FL, 2006, April 3-6, 2006, pp. 395-406.

[5] T. Zedníček. New Tantalum Capacitor Technologies Polymer and NbO. *AVX Technical information*. 2007, Available: https://www.avx.com/docs/techinfo/New_Tantalum_Technologies.pdf

[6] A. Teverovsky, "Scintillation and Surge Current Breakdown Voltages in Solid Tantalum Capacitors," *IEEE Transactions on Dielectrics and Electrical Insulation*, vol. 16, pp. 1134-1142, 2009

[7] Y. Jin, Q. Chen, and P. Lessner, "Thermal Stability Investigation of PEDOT Films from Chemical Oxidation and Prepolymerized Dispersion," *Electrochemistry*, vol. 81, pp. 801-803, 2013

[8] K. T. Jacob, A. Kumar, G. Rajitha, and Y. Waseda, "Thermodynamic Data for Mn3O4, Mn2O3 and MnO2," *High Temperature Materials and Processes*, vol. 30, pp. pp. 459–472, 2011

[9] M. Hedden, N. Francis, J. T. Haraldsen, T. Ahmed, and C. Constantin, "Thermoelectric Properties of Nano-Meso-Micro β-MnO2 Powders as a Function of Electrical Resistance," *Nanoscale research letters*, vol. 10, pp. 1000-1000, 2015

[10] X. W. J. Liu, D. Li, N.E.Coates, R.A.Segalman, D.G.Cahill, "Thermal Conductivity and Elastic Constants of PEDOT:PSS with High Electrical Conductivity," *Macromolecules*, vol. 48, pp. 585-591, 2015

[11] R.Holm, *Electrical Contacts, Theory and Applications*: NewYork, Springer-Verlag, 1967.

[12] J. H. Yu, G. De Temmerman, R. P. Doerner, R. A. Pitts, and M. A. van den Berg, "The effect of transient temporal pulse shape on surface temperature and tungsten damage," *Nuclear fusion*, vol. 55, p. 93027, 2015

[13] D. Lelmini and R. Waser, *Resistive Switching: From Fundamentals of Nanoionic Redox Processes to Memristive Device Applications*: Wiley-VCH Verlag GmbH & Co. KGaA 2016.

[14] H.Chee, T.Kumar, and H.Almurib, "Electrical model of multi-level bipolar Ta2O5/TaOx Bi-layered ReRAM," *Microelectronics Journal*, vol. 93, p. 104616, 2019

[15] X. X. Zhang, Ling; Zhang, Hui; Liu, Jian; Tan Dingwen, "Effect of Joule Heating on Resistive Switching Characteristic in AlOx Cells Made by Thermal Oxidation Formation," *Nanoscale Research Letters*, vol. 15, 2020

[16] A. Teverovsky, "Degradation of leakage currents in solid tantalum capacitors under steady-state bias conditions," in *Electronic Components and Technology Conference (ECTC), 2010 Proceedings 60th*, 2010, 1-4 June 2010, pp. 752-757.

[17] A. Teverovsky, "Anomalous Transients in Chip Polymer Tantalum Capacitors," presented at the ESA 3rd International Symposium - Space Passive Component Days, Noordwijk, The Netherlands, 2018. https://www.spcd.space/

[18] D.Smith, "Solid-State Anodic Oxidation of Tantalum," *Journal of the Electrochemical Society, 1966, Volume: 113 Issue: 1 Page: 19*, vol. 113, pp. 19-25, 1966